WATER RESOURCES RESEARCH, VOL. 44, W12413, doi:10.1029/2008WR006964, 2008

# Developing and applying uncertain global climate change projections for regional water management planning

David G. Groves,[1] David Yates,[2] and Claudia Tebaldi[3]

Received 24 February 2008; revised 10 August 2008; accepted 8 September 2008; published 10 December 2008.

[1] Climate change may impact water resources management conditions in difficult-to-predict ways. A key challenge for water managers is how to incorporate highly uncertain information about potential climate change from global models into local- and regional-scale water management models and tools to support local planning. This paper presents a new method for developing large ensembles of local daily weather that reflect a wide range of plausible future climate change scenarios while preserving many statistical properties of local historical weather patterns. This method is demonstrated by evaluating the possible impact of climate change on the Inland Empire Utilities Agency service area in southern California. The analysis shows that climate change could impact the region, increasing outdoor water demand by up to 10% by 2040, decreasing local water supply by up to 40% by 2040, and decreasing sustainable groundwater yields by up to 15% by 2040. The range of plausible climate projections suggests the need for the region to augment its long-range water management plans to reduce its vulnerability to climate change.

**Citation:** Groves, D. G., D. Yates, and C. Tebaldi (2008), Developing and applying uncertain global climate change projections for regional water management planning, *Water Resour. Res.*, *44*, W12413, doi:10.1029/2008WR006964.

## 1. Introduction

[2] Climate change is important to water planners and managers because it may change underlying water management conditions [*Barnett et al.*, 2008; *Intergovernmental Panel on Climate Change* (*IPCC*), 2007a] and increase the need for new water management programs and capital investments [*California Urban Water Agencies*, 2007]. Climate change may also confound water resources planning because the local effects of climate change are so uncertain and difficult to predict [*Knopman*, 2006; *Miller and Yates*, 2006; *Stakhiv*, 1998]. The most reliable information about how the climate may change is available on coarse geographical scales, whereas water managers must respond to changes that occur at the local and regional level [*Kim et al.*, 1984; *Lamb*, 1987]. A key challenge for water managers is how to incorporate potentially-significant and highly uncertain information about potential climate changes into available water management models and tools to support local management decisions.

[3] Studies have shown that it is important to include the effects of climate change in local water planning [*Schimmelpfennig*, 1996]. *Risbey* [1998], seeking to link present-day planning decisions to uncertain future climate projections, for example, performed a qualitative sensitivity analysis that showed that water-planning decisions were sensitive to uncertainty in the range of global climate model simulations for the Sacramento basin in California. More recently, researchers have used integrated water resource planning models to evaluate the impact of climate perturbations on the performance of current water management systems [*Brekke et al.*, 2004; *Vicuna et al.*, 2007; *Zhu et al.*, 2005].

[4] The most comprehensive projections of future global climate conditions are provided by atmosphere-ocean general circulation models (AOGCMs). Problematically to water planners, however, outputs from AOGCMs are typically available at spatial scales of 100 kilometers or more. Furthermore, different AOGCMs run under the same greenhouse gas emissions forcing scenario can produce profoundly different projections of temperature and precipitation change, particularly at the regional scale (see chapter 10 of *IPCC* [2007b] for a comprehensive discussion of AOGCM predictions).

[5] In order to directly evaluate how global projections of climate change will impact local or regional water agencies, water planners will need climate change information at spatial scales comparable to their service area and the source regions of their supplies. A commonly-used approach is to statistically "downscale" individual AOGCM model results to a local scale. In general, the primary goal in downscaling is to post-process the AOGCM output so that it reflects the large-scale features and temporal trends from the AOGCM simulation, but also the historical patterns of climate variables at the regional and local scale [*Fowler et al.*, 2007; *Wood et al.*, 2004]. This is typically done by developing a statistical relation between atmospheric quantities characterizing large-scale processes (e.g., height of the 500 millibar (mb) atmospheric pressure field) and those local quantities that are relevant to a watershed manager (e.g., precipitation and temperature at specific locations in the watershed). Other methods include bias-correcting AOGCM data to more

[1]Infrastructure, Safety, and Environment, RAND Corporation, Santa Monica, California, USA.
[2]Research Applications Laboratory, National Center for Atmospheric Research, Boulder, Colorado, USA.
[3]Climate Central, Princeton, New Jersey, USA.


0043-1397/08/2008WR006964$09.00

closely match regional climate, and then spatially disaggregating the data to the local scale [*Maurer*, 2007].

[6] There are several limitations to traditional downscaling procedures. For example, while AOGCMs are able to simulate large-scale climate features realistically, they typically exhibit important biases at regional-scales, which is problematic for analysis of implications of climate change for hydrology and water resources [*Maurer*, 2007; *Wood et al.*, 2004]. Another challenge is that the downscaling procedure produces individual weather sequences corresponding to single AOGCM model runs, restricting the number of weather sequences developed. As AOGCMs produce significantly different climate change responses, a water manager is left to wonder which downscaled climate scenarios to use and if the available runs represent all the plausible projections of interest. As these downscaling methods do not allow for the development of other variants of the AOGCM run-specific weather sequences, one cannot evaluate the implications of droughts that occur at times different than those projected by the specific AOGCM simulation.

[7] Another approach is to develop weather generators that synthetically create new sequences of weather that are statistical similar to historical climate and include other imposed trends [*Kilsby et al.*, 2007]. This method, however, requires the development of a new statistical model appropriate for each location in which weather sequences are sought. For regions in which these relationships have not yet been developed, significant new analysis is required, a task that is likely outside the expertise of many water agency planners.

[8] This paper proposes an approach that generates synthetic sequences of local weather data (e.g., temperature and precipitation) that reflect both local weather variability and regional trends projected by AOGCMs. This approach relies on a methodology that combines predictions from individual AOGCMs into a single probabilistic climate projection for a region of interest using the criteria of bias and convergence [*Tebaldi et al.*, 2005]. Such probabilistic regional projections are then used to guide a K-nearest neighbor (K-nn) bootstrapping technique [*Yates et al.*, 2003] to develop an arbitrarily-large number of individual weather sequences that have the same statistical characteristics of local weather but are consistent with the range of AOGCM-derived temperature and precipitation trends.

[9] This generic approach enables an analyst to develop any number of weather sequences that reflect uncertainty about the effects of climate change uncertainty to use with local or regional water management models. The paper concludes by demonstrating how this climate information can be incorporated into a hydrologically-based water planning model using a case study of the Inland Empire Utilities Agency (hereafter, IEUA), a water and wastewater wholesaler in southern California. The case study suggests that this method could have broad applicability to local water utilities and regional water assessments both in the US and abroad.

## 2. Creating Local Climate Change Scenarios From Coarse-Scale AOGCMs

[10] Determining plausible ranges and likelihoods of global climatic changes has flourished as a research topic in recent years [*Pittock et al.*, 2001; *Tebaldi et al.*, 2004, 2005; *Yates et al.*, 2003]. Some of this work has been based on energy balance or reduced climate system models that run quickly and can be evaluated under many different configurations and parameterizations to develop ensembles of results. However, these low-dimensional models do not extend in a straightforward way to small-scale regional and local climate change analyses because of the observed spatial heterogeneity of past climate and, by inference, projected future changes. This is particularly problematic in the water resources planning arena, as it is at the local and regional scale where climate change impacts will express themselves. However, recent coordinated efforts, in which numerous higher-resolution, fully-coupled climate models have been run for a common set of experiments, have produced large data sets that can be used to generate probabilistic estimates of future climate at global and regional scales.

### 2.1. Ensemble Climate Projections From AOGCMs for Southern California

[11] There are two main approaches for combining the results of many AOGCMs (i.e., multimodel ensemble output) for purposes of driving climate impact assessment models. One simply considers each model as equal and produces ensemble averages and measures of inter-model variability (e.g., standard deviation and range). The other, formalized by several published methods, weights model results unequally based on different measures of model merit. For example, the Reliability Ensemble Average (REA) approach [*Giorgi and Mearns*, 2002] weighs more heavily models that are characterized by small bias in modeling historical climate (in terms of multidecadal averages of regionally and seasonally aggregated temperature and precipitation) and that agree with the ensemble ‘‘consensus’’. This approach motivated the work of *Tebaldi et al.* [2004, 2005].

[12] *Tebaldi et al.* [2005] derived regional probability distributions of future climate from the output of individual AOGCMs using a fully Bayesian approach to combine the predictions of the individual forecasts into a single probabilistic forecast which formalizes as a consequence of the statistical assumptions the REA criteria of bias and convergence. A posterior distribution of the climate signal is developed using historical data and the AOGCMs’ projections. An initial prior distribution, chosen to be non-influential (i.e., one that is ‘‘flat’’ over a wide range of possible values for the future temperature or precipitation change), is updated numerically using Bayes’ theorem to account for the observed record and the ‘‘new’’ observations of the future conditions as estimated by individual AOGCMs. In the posterior estimate of the climate change signal, the AOGCMs that perform well in recreating recent climate (low bias) and that show convergence (i.e., contribute to the consensus in the future trajectories) are weighted more heavily. Recognizing that current AOGCMs are not completely independent, this method treats the convergence criterion less stringently [*Tebaldi et al.*, 2004]. Also, as a consequence of the fundamental lack of correlation between the size of the model bias and the magnitude of its projected change, the derived probability density functions (PDFs) do not differ significantly from a smoothed histogram of the original model projections of change, with the mode of the

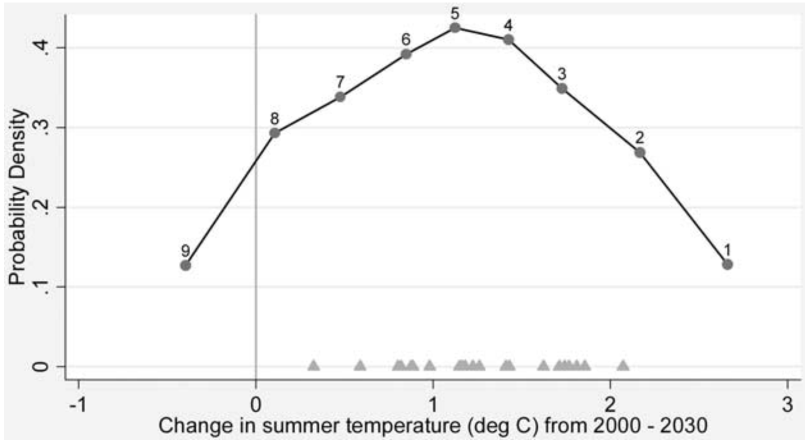


**Figure 1.** Probability density function of summer temperature change between 2000 and 2030 for the A1B SRES scenario and the southern California region. Points on the curve refer to the deciles of the PDF. Triangles indicate trends from the individual AOGCMs.

PDF close to the simple ensemble mean. Other methods have been proposed that combine multimodel ensembles into probabilistic projections either at the model grid scale [*Furrer et al.*, 2007] or at large, subcontinental regional scales [*Greene et al.*, 2006]. The method by Tebaldi et al. has been further developed by *Smith et al.* [2008] and is easily adapted to any arbitrarily shaped and sized region.

[13] For this study we use the climate simulation results from twenty-one state-of-the-art AOGCMs from the World Climate Research Programme's (WCRP's) Coupled Model Intercomparison Project phase 3 (CMIP3) multimodel data set (available from http://www-pcmdi.llnl.gov/ipcc/about_ipcc.php). Standardized experiments have been run using these models under different scenarios of future greenhouse gas emissions, and we use the AOGCM results from the A1B scenario—a mid-range emissions scenario whose trajectory can be defined close to a "business as usual" scenario [*IPCC*, 2000]. It is important to note that for the next several decades, the atmospheric greenhouse gas concentrations do not significantly differ in response to different emissions trajectories.

[14] In our case study of the IEUA service area, we area-average the seasonal surface temperature and precipitation projections from each AOGCM for the four grid points covering the southern California area for a baseline period (1980–1999) and two future periods of interest (2020–2039) and (2040–2059). We use 20-year averages in order to isolate as much as possible (1) the signal of change caused by the externally forced change in GHG concentration from (2) the signal of multidecadal variability that may be present in the model projections. This is especially relevant for the shorter "forecast" time, when GHG concentrations are not much higher compared to that of the baseline period. We then applied the Bayesian model that combines area-averaged values into probability distribution functions of temperature and precipitation change.

[15] Figures 1 and 2 show PDFs of summer (June, July, and August) temperature change (in degrees C) and winter (December, January, and February) precipitation change (in percent precipitation change) from the baseline period (1980–1999) to 2030. The individual changes as estimated by each AOGCM are indicated by a triangle on the x-axis (biases of the individual models used in the Bayesian

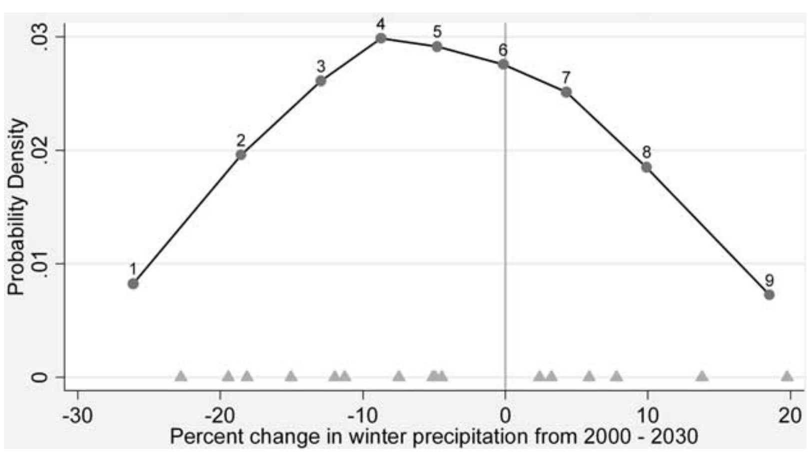


**Figure 2.** Probability density function of winter precipitation change between 2000 and 2030 for the A1B SRES scenario and the southern California region. Points on the curve refer to the deciles of the PDF. Triangles indicate trends from the individual AOGCMs. One model outlier exists at +45%.

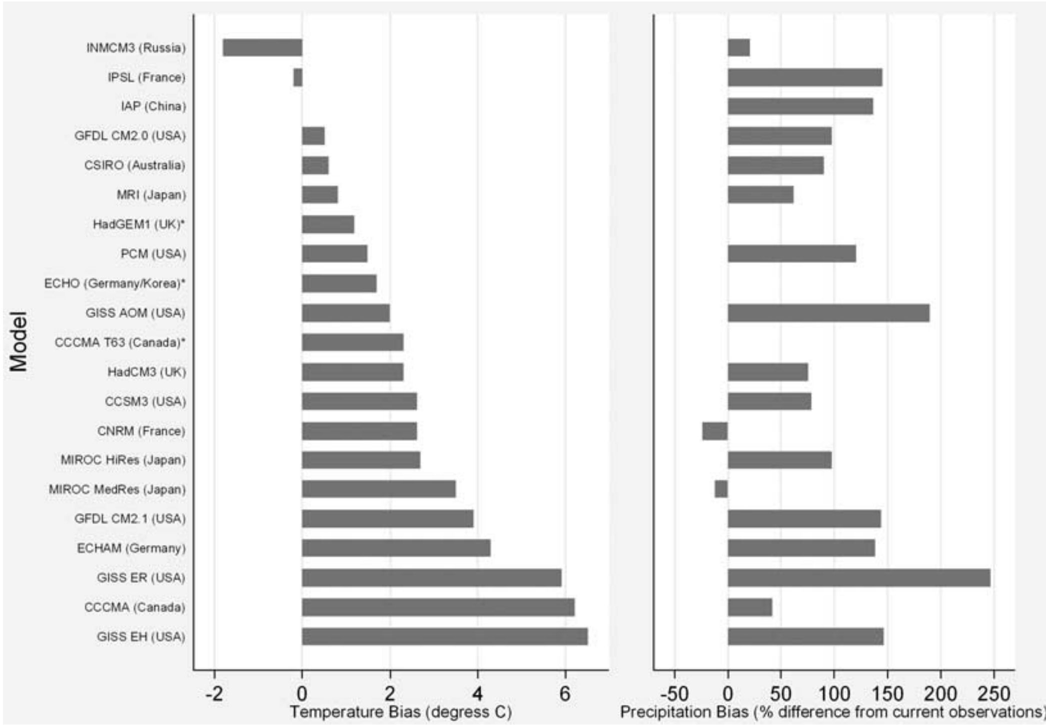


**Figure 3.** AOGCM model biases in terms of (left) summer (JJA) average temperature (in degrees centigrade) and (right) winter (DJF) average precipitation (in percentage difference from current observations). The asterisks indicate the three models that are used only for the temperature analysis.

analysis—which are not correlated to the projected changes reflected in the PDFs—are shown in Figure 3). Figure 1 shows a range of projected summer temperature change between slightly below zero to over two degrees Celsius. The winter precipitation changes predicted by the individual AOGCMs range from a 25% decrease to a 20% increase (although there is one outlier result that projects a 45% increase). The resulting densities indicate a stronger consensus of drier winter conditions relative to the current climate. The outcome of the combined AOGCM projections for precipitation change is typical of many regions, particularly in mid-to-low latitudes, where there is low agreement among the different models [*IPCC*, 2007b].

[16] Note that the Bayesian model is run separately for both precipitation and temperature, and does not provide joint probabilistic projections. A regression analysis of 16 AOGCM projected annual temperature and annual precipitation trends over the study area from 2005–2050 (for the A1b emissions scenario) shows a weak, statistically insignificant negative correlation ($p = 0.323$). When two of the 16 temperature trend and precipitation trend pairs are excluded, however, the negative relationship become highly significant ($p = 0.000$). Following this suggestive evidence, we assumed that temperature and precipitation trends will be negatively correlated, and so the driest (wettest) range of the precipitation trends corresponds to the warmest (coolest) temperature trends. This assumption is conservative, in that it will lead to the most inclusive set of plausible climate scenarios as a basis of testing the water-management plans of the IEUA region.

### 2.2. Generating Local Climate Sequences From the Regional Densities Using K-nn

[17] We next use these regional climate change distributions to develop information relevant for a regional water resource planning model. The technique presented here uses the output from the Bayesian method to condition a K-nearest neighbor (K-nn) resampling scheme that generates daily weather sequences yielding ensembles of alternative climate data [*Yates et al.*, 2003]. The K-nn algorithm produces daily weather variables at multiple stations within the region covered by the AOGCM grid boxes used to develop the trend distribution. The derived weather sequences preserve the spatial and temporal dependencies and important cross correlations and autocorrelations of the local historical weather while reflecting large-scale climate trends from the Bayesian model. This technique allows for the creation of ensembles of local climate scenarios that can be used in a water planning model for addressing the potential impacts of climate change and climate variability, placed within an uncertainty analysis framework.

[18] K-nn creates new, synthetic weather sequences by resampling the historic daily data set in such a way that the statistical properties of the observed weather data are preserved. The K-nn Step 1 selects a random starting calendar day; say a 1 January from all $N$ available 1 January. Step 2 defines a window of days, $w$ to the left and right of the starting day selected in Step 1, and aggregates the daily weather station data into a regional mean. The regional mean is used to find candidate days similar to the day chosen in Step 1, where similarity is based on a Mahalanobis distance measure (see *Yates et al.* [2003] for details).

**Table 1.** A Portion of the Ranked List of Regional Precipitation Anomalies by Week and Year[a]

| Categorical Year | $I_w^N$ | Week 1 | Week 2 | ... | Week 52 |
|---|---|---|---|---|---|
| 1; dry | Year 1 | 1981 | 1983 | ... | 1980 |
| 2; dry | Year 2 | 1983 | 1984 | ... | 1985 |
| ... | ... | ... | ... | ... | ... |
| *N*; wet | Year 24 | 1995 | 1993 | ... | 1994 |

[a]See text for details.

With a window width of $w$ = 7 and a data set with $N$ = 24 years, the total number of candidate days then given as $k = \sqrt{[(2w+1) \times N]} - 1$ or $k$ = 19 [*Rajagopalan and Lall*, 1999]. One of the $k$ similar days is then randomly selected (Step 3), and represents a day similar to 1 January selected in Step 1. The subsequent day to this selected day is used as the successor, leading to a new 2 January (Step 4). The window of days is then shifted one day to the right, and Steps 2 through 4 are repeated. Successive iterations of these steps then generate new, unique daily time series that have many of the same statistical properties such as autocorrelation, cross-covariance, and mean value as the original data [*Yates et al.*, 2003].

[19] To reflect a changing climate, as suggested by the Bayesian climate trends, the pool of "similar days" from which the next day is selected can be biased to include more warm/cold or wet/dry days. Biased resampling requires a conditioning criterion to select a subset of years, $n \in N$, that will be used in the K-nn algorithm. The simplest criterion would be some large-scale climate signal such as the El Nino/Southern Oscillation (ENSO) index, where only years with a particular ENSO attribute would comprise the $n \in N$ subset (e.g., only resample from days of daily data). This approach would work fine for short weather sequences, such as a year; but for longer sequences, it would be desirable to dynamically select an $n$ subset from the population of $N$ years so that longer weather sequence could reflect different climate regimes. To do this, a temporal, probabilistic resampling scheme is introduced that generates a subset of days for each week $w$ of year $t$ whose days have a higher or lower probability of being selected based on a weighting criterion.

[20] The weighting criterion is based on a table of weekly climate anomalies, estimated from historic climate data. These weekly anomalies are assigned a ranked index, $I_w^N$, for all weeks $w$ and years $N$. Table 1 shows an example of this ranking using precipitation data from the IEUA service area (from 1980 to 2003), where regional precipitation anomalies are ranked from driest to wettest. For example, in the 24 years of observational data, the driest week 1 (e.g., the period 1 through 7 January) was 1981, while the wettest week 1 was 1995. The driest week 2 was the year 1983, while the wettest week 2 was 1993; and so on.

[21] To generate the $n_w^t$ subset, an index function is used to randomly generate indices ranging from $i$ = 1 to $N$,

$$I_w^i = INT\left[N\left(1 - u^{\delta_w^i}\right)\right] + 1 \tag{1}$$

where $u$ is a uniform random number, $U(0, 1)$ and $\delta_w^i$ is a weighting parameter that is used to bias years in the ranked list. In Table 1, years are ranked from driest, with an index value of 1, to wettest, with an index value of $N$. A weight parameter, $\delta_w^i$ = 1.0, means each year has an equal probability of making up the $n_w^t$ subset, values greater than 1.0 will tend to bias the selection of wet years, while weight parameter values less than 1.0 will tend to bias dry years. The weight parameter, $\delta_w^i$ of equation (1) can be estimated both by week (intra-annual change) and by year (inter-annual change). With a given set of $\delta_w^i$ weights, equation (1) can be randomly queried, leading to a set of indices that correspond to particular years from the ranked list. Finally, this yields a set of biased years, $n_w^t$ from which K-nn can resample.

[22] The AOGCM-based Bayesian estimate of changes in seasonal precipitation ($\Delta P'^i_s$) and temperature ($\Delta T'^i_s$) for southern California were linearly interpolated into weekly time series, $\Delta P'^i_w$ and $\Delta T'^i_w$ from 2000 to 2060. These interpolations were made for the nine discrete intervals and for each of the four seasons (see Figures 1 and 2). These were then used to establish the weighting parameter, $\delta_w^i$ for conditioning K-nn, where $\delta_w^i = \alpha_w \Delta P'^i_w + \beta_w \Delta T'^i_w$. The $\alpha_w$ and $\beta_w$ coefficients were determined by trial-and-error to minimize the difference between the Bayesian estimates of climate change and the difference between the future synthetic climate and the mean regional climate from the historic record. For precipitation, this can be expressed as,

$$\min\left[\Delta P'^i_s - \left(\frac{1}{K}\sum_{i=1}^{K} \widehat{P}^i_s - \widehat{Po}_s\right)\right] \tag{2}$$

where the regional mean total precipitation for year $i$ and season $s$ is:

$$\widehat{P}^i_s = \frac{1}{m}\sum_{j=1}^{m} \widehat{P}^i_{j,s} \tag{3}$$

and $\widehat{P}^i_{j,s}$ is the season total precipitation for station $j$ and year $i$; while $\hat{P}o_s$ is the seasonal station mean computed from the observations. The total number of stations is $m$ and $K$ is the number of synthetic sequences generated by K-nn. Figure 4 shows the final weights, $\delta_w^i$, and the corresponding change in precipitation from the Bayesian model for two select deciles: 2 and 8.

[23] For the case of the IEUA, $N$ = 24 years of daily weather data (1980 through 2003) for $m$ = 11 stations were used to generate biased daily weather sequences with K-nn, conditioned off the results from the Bayesian analysis [*Thornton et al.*, 1997]. For nine deciles of the distributions shown in Figures 1 and 2, 20 realizations were made leading to a total of 180, 60-year time series. Note that realizations are assigned a decile based on the temperature and precipitation trend applied in the conditioning. Because of the stochastic factors in the K-nn analysis, the precipitation and temperature trends for individual realizations may not always order according to a decile. For example, some decile 3 realizations may have larger temperature trends than some deciles 2 realizations.

[24] Figures 5 and 6 compare the K-nn simulated data, the AOGCM ensemble results, and the historical data for

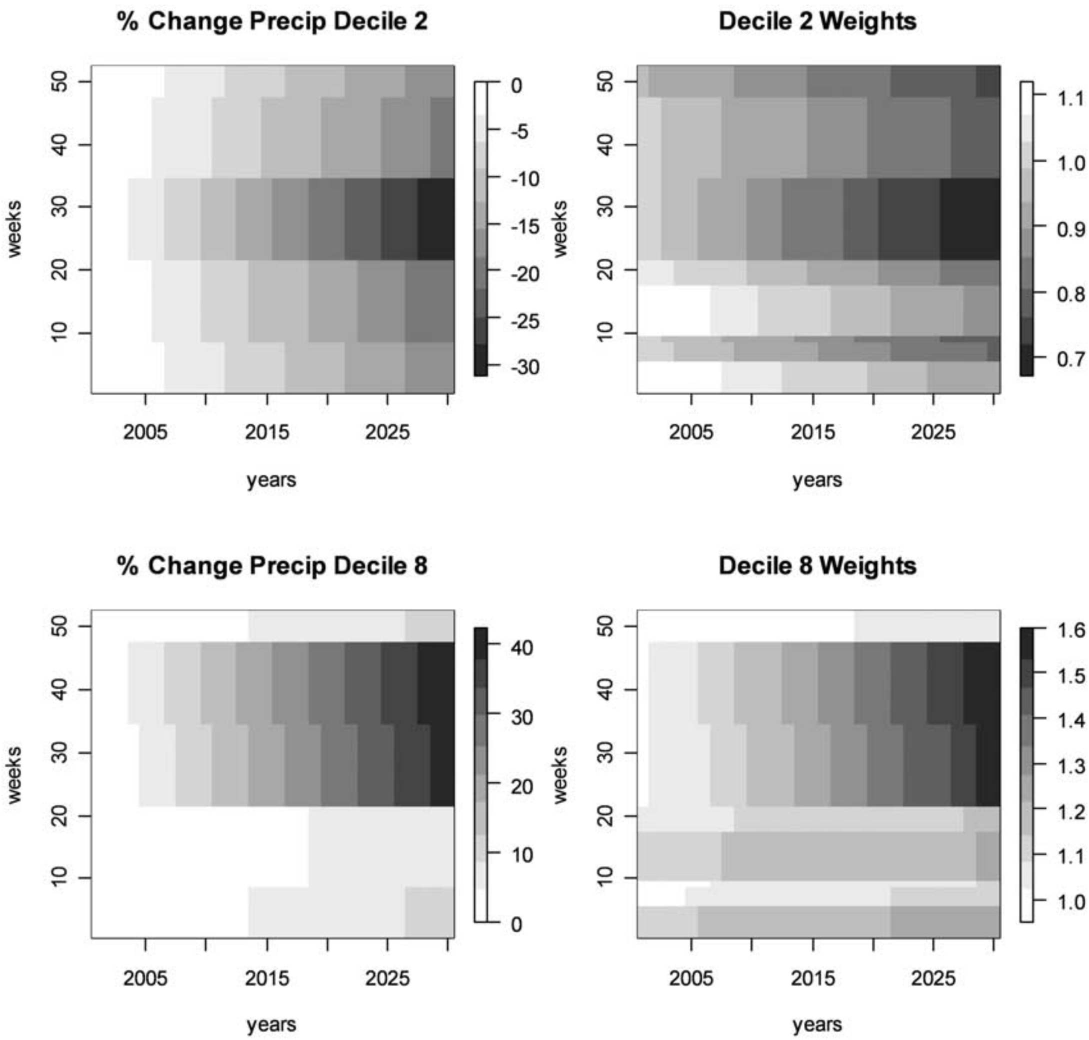


**Figure 4.** (Left) Percentage change in precipitation for (top) decile 2 and (bottom) decile 8 and the (right) final weights used by K-nn to condition the resampling process by month (vertical axis) and year (horizontal axis).

three discrete deciles (1, 5 and 9) of the Bayesian trend distributions for winter precipitation and season temperature. The data from the entire historical period can be summarized as a single box plot, which is shown on the left portion of the graph as total seasonal precipitation (Figure 5) and temperature (Figure 6) averaged over the region. These box plots represent the range of precipitation and temperature present in the sample of historical data, and should be compared with box plots to the right that summarize each year of simulated data. Linear and nonlinear (e.g., loess—see *Cleveland and Devlin* [1988]) trends in the historical data indicate a decrease in winter precipitation and an increase in summer temperatures throughout the brief historical period.

[25] The right portion of each figure includes box plots that summarize the simulated data for precipitation and temperature for a select set of deciles. Each individual box plot summarizes all 20 realizations created for a given year. The variance within these values is approximately equivalent to that of the historical data. The thick, light lines in the figures depict the linear trend from the Bayesian analysis, while the dark line is the mean of all 20 realizations. Values of $\delta_w^i$ were chosen so these lines closely matched (e.g., the minimization expressed in equation (2)). Note that decile 1 corresponds to the "very-warm and dry" scenarios, while decile 9 are the "warm and wet" scenarios. Also worth noting, the variance within each simulated series remains about constant throughout each time series realization.

[26] Figure 7 shows three representative sequences of summer temperature and winter precipitation from 1980 to 2060. The data from 1980 to 2003 are based on historical data. The data from 2004 to 2060 are based on three realizations of the K-nn procedure, corresponding to a range of conditioning trends.

## 3. Utilizing the Local Weather Sequences in a Water Management Model

[27] The local weather sequences created using the Bayesian-K-nn method can be used with an integrated water resource management (IWRM) model to evaluate the impact of climate change on a water management system. The literature is rich with IWRMs that have tended to focus on

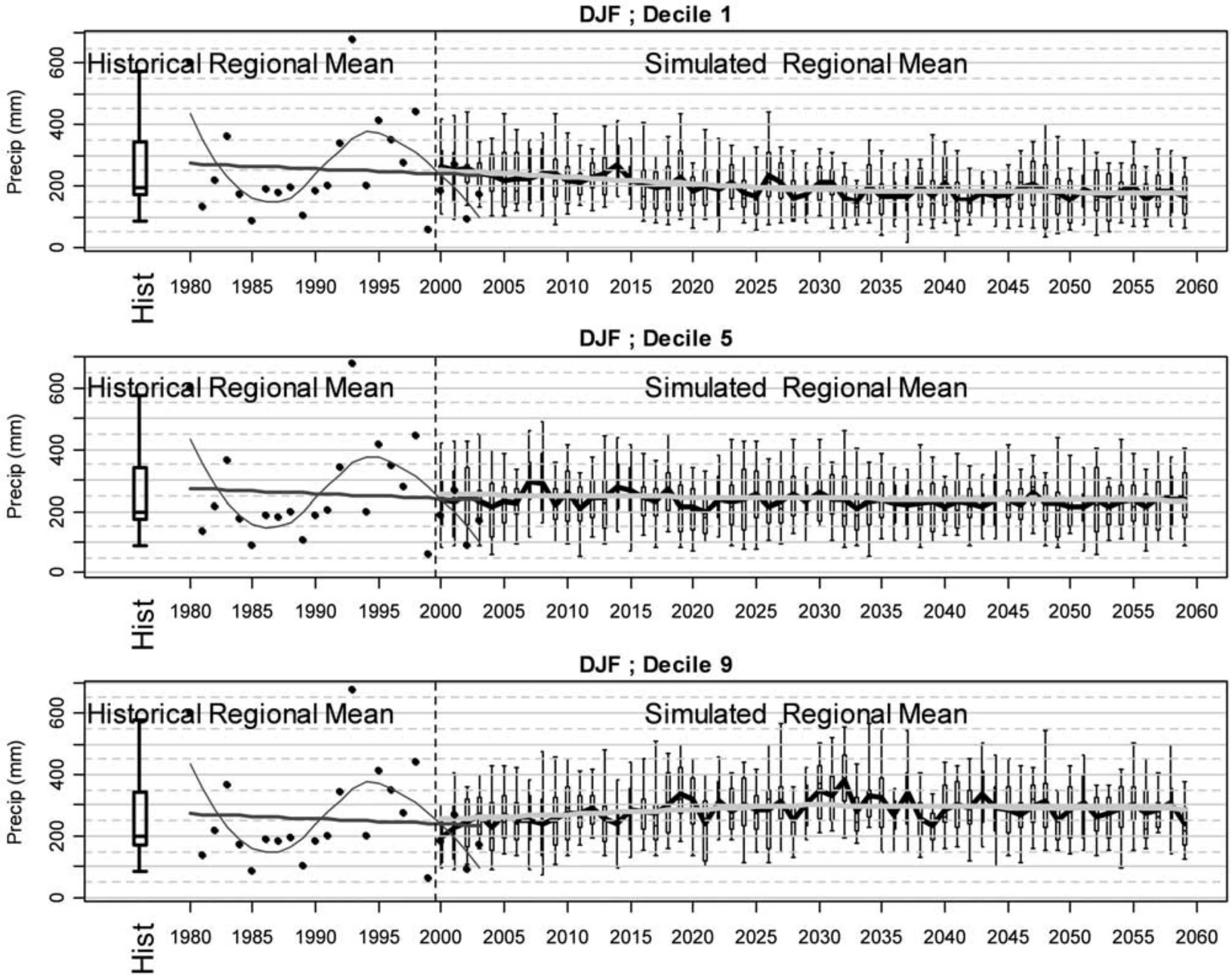


**Figure 5.** Winter precipitation (December, January, and February) for the historic period (1980 through 2003) with a (left graph) trend and loess lines and summarized as a (far left) box plot. Right portion of graph are the K-nn simulated time series of annual precipitation, given as box plots for all realizations ($K = 20$). The thick, light-colored line is the AOGCM ensemble climate change estimate relative to the historic mean.

either understanding how water flows through a watershed in response to hydrologic events or on allocating the water that is available in response to those events. The Water Evaluation and Planning Version 21 (WEAP) IWRM (available from http://www.weap21.org) attempts to address the gap between water management and watershed hydrology by integrating a range of physical hydrologic processes, including rainfall-runoff and snow physics, with the management of demands and installed infrastructure by simulating the water balance for a user-constructed, link-and-node representation of a water management system [*Yates et al.*, 2005a, 2005b]. WEAP allows for multiple-scenario analysis, reflecting uncertainty about climate change and anthropogenic stressors, such as land use variations, changes in municipal and industrial demands, alternative operating rules, and points of diversion changes. Of particular interest to this study, WEAP can evaluate the impact of alternative sequences of local weather conditions (e.g., temperature, precipitation, humidity, and wind speed) on soil moisture and irrigation requirements, surface and subsurface rainfall runoff, and percolation of precipitation and irrigation into aquifers. The WEAP IWRM has been applied to numerous watersheds and districts throughout the world, including the Sacramento Valley, in California [*Yates et al.*, 2008]. *Huber-Lee et al.* [2006] provide additional background on WEAP and present three municipal water case study applications.

## 4. A Case Study of the Inland Empire Utilities Agency in Southern California

[28] To demonstrate how the climate change data derived from the Bayesian-K-nn approach described above can be utilized in a water planning model to inform water planning decisions, we present a case study focused on the service area of the Inland Empire Utilities Agency (IEUA), a wholesale water and wastewater provider in Riverside County, southern California (Figure 8). This analysis represents a subset of work performed in collaboration with IEUA staff members and focuses on illustrating the range of impacts that climate may have on the water system. Work examining new approaches to interpreting this information

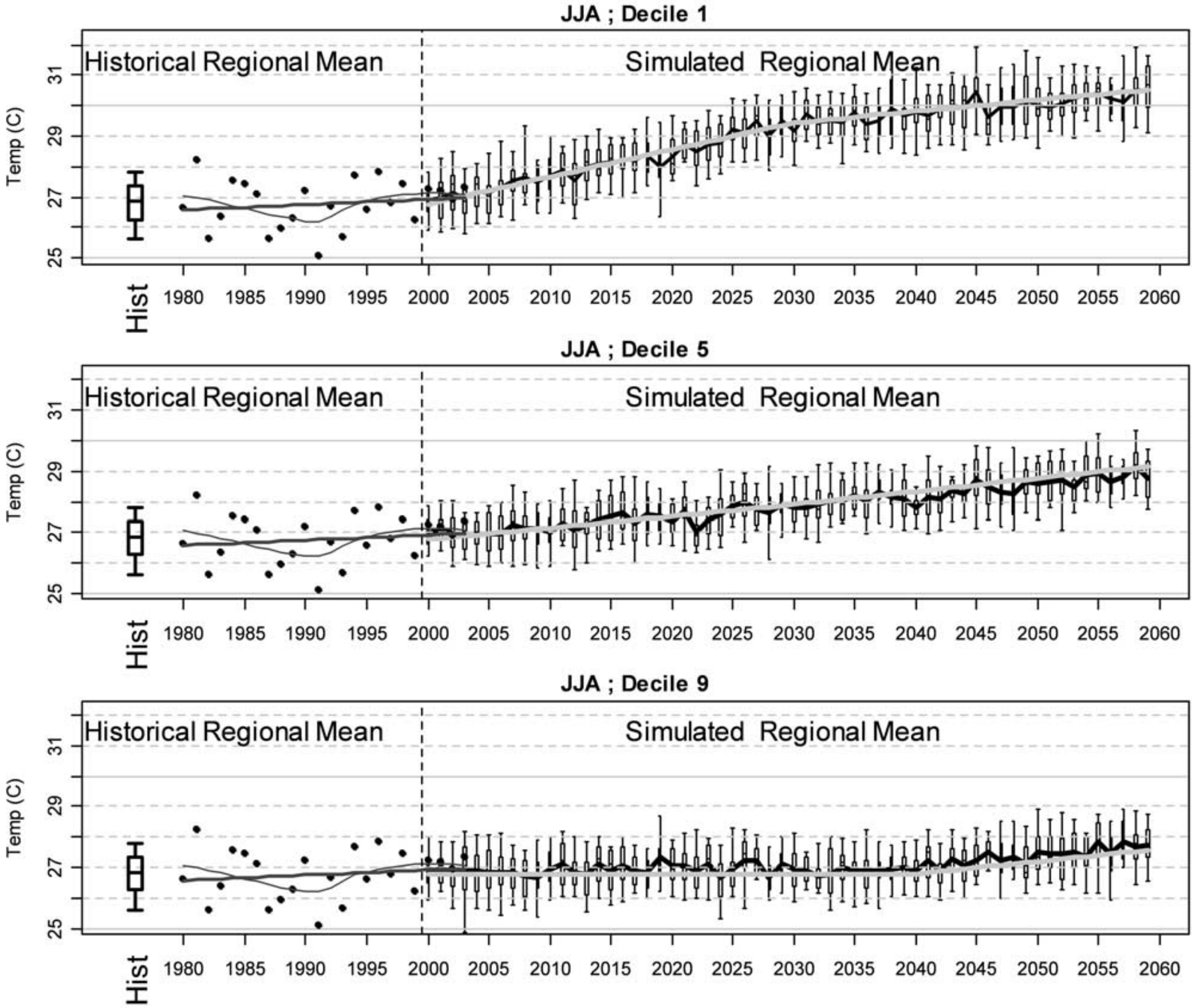


**Figure 6.** Same as Figure 5 but for average summer temperature (June, July, and August).

for decision making is presented by *Groves et al.* [2008a, 2008b].

[29] The IEUA region is in the midst of rapid urban growth and transformation from an agricultural region dominated by dairy farms to industrial and planned residential developments. It is projected that the region's population of 800,000 will grow to approximately 1.2 million by 2025, placing new demands on the water supply and wastewater treatment system [*IEUA*, 2005].

[30] The IEUA region currently meets slightly more than half of its average water needs from groundwater sources within the region (primarily the underlying Chino Groundwater basin aquifer), about a quarter from Northern California via a large intra-state water distribution system (i.e., the California State Water Project), and the rest from local rivers and streams and a rapidly expanding recycled water system [*IEUA*, 2005]. The Chino Groundwater basin was adjudicated in 1978 [*Chino Basin Municipal Water District v. City of Chino*, 1978] and is managed to maximize sustainable extractions of groundwater according to the Chino Basin Optimum Management Program (OBMP) [*Wildermuth Environmental*, 1999]. Two key components of the groundwater program are (1) a comprehensive program to replenish the groundwater basin with imported, recycled, and local storm water and (2) limitations on extractions to ensure long-term sustainability. The management plan stipulates that allowable extractions will be adjusted over time to respond to changing groundwater conditions.

### 4.1. Plausible Impacts of Climate Change to the IEUA Region

[31] A simple qualitative assessment of the region's system would suggest that climate change has the potential to impact water supply reliability by increasing irrigation demands, decreasing the natural recharge of the groundwater basin that would lead to more stringent restrictions on groundwater use, decreasing local runoff and derived municipal supplies, and reducing the availability of imported water from Northern California.

[32] To quantitatively assess the ranges of plausible impacts that climate change may have upon water manage-

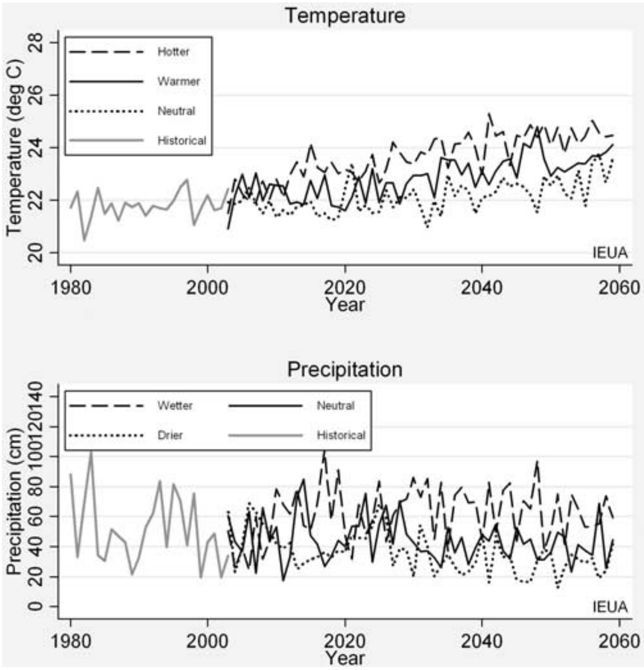


**Figure 7.** Representative temperature and precipitation sequences for the IEUA region derived using K-nn conditioned to recreate the extremes of the regional trend PDFs.

ment in the IEUA service area, we developed a WEAP model that estimates the performance of IEUA's water management strategies under each of the future weather sequences produced by the Bayesian-K-nn procedure described above. To automate the generation and management of a large number of WEAP simulations corresponding to the developed climate change weather sequences (or scenarios), we used the Computer Assisted Reasoning system (CARs™), available from Evolving Logic (www.evolvinglogic.com).

[33] The WEAP model was designed to produce under nominal assumptions results that are consistent with the various IEUA estimates of water demand and supply included in the IEUA 2005 Regional Urban Water Management Plan (hereafter, IEUA RUWMP) [*IEUA*, 2005]. The WEAP model necessarily simplifies a complex water management system and thus assessed climate impacts may be biased. The ultimate purpose of the analysis, however, was to develop and illustrate new approaches for addressing climate uncertainties in water planning—not necessarily to develop the most comprehensive or accurate model representation of the case study area.

[34] The WEAP model simulates water supply and demand using a stylized representation of the major water flows of the system on a monthly time scale from 2005 to 2040. The model represents supply and demand relationships by using a set of nodes corresponding to discrete water management elements such as catchments, indoor-demand sectors, surface supplies, and groundwater basins. These elements are linked together by rivers, conveyance facilities, and other pathways (such as percolation flows).

[35] The model includes a simple representation of the Chino Groundwater basin aquifer in which "effective safe yield" for pumping and direct use is endogenously calculated at 5-year intervals throughout the simulation such that groundwater inflows (e.g., percolation from overlying catchments and replenishment by imported, recycled, and


**Figure 8.** Map of the IEUA service area, California, USA. The city of Ontario is located at 34°N, 117°41′W.

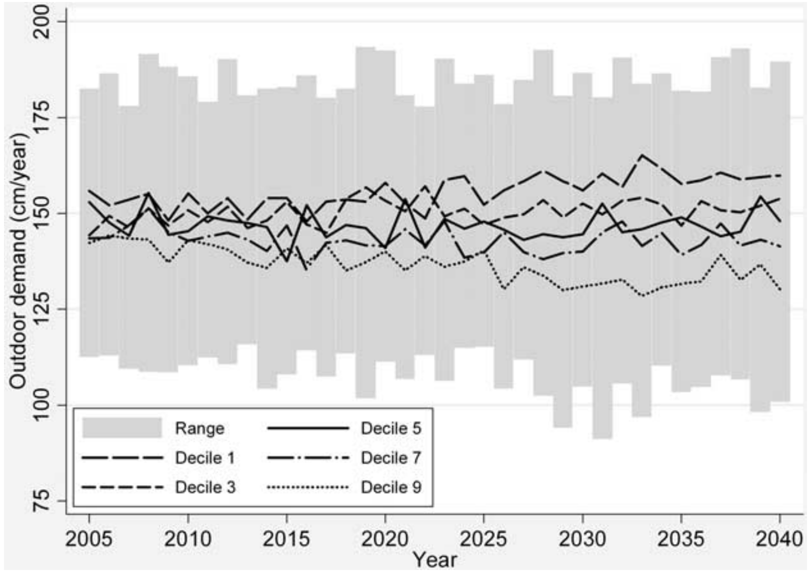


**Figure 9.** Projected outdoor water demand (in centimeters per year) for the IEUA region under different weather sequences consistent with the climate change projections from the AOGCMs. The lines indicate averages over 20 sequences for deciles 1, 3, 5, 7, and 9. The shaded bars indicate the entire range of annual demand per year. Note that the deciles are defined based on the conditioning precipitation and temperature trends used in the K-nn procedure. They are not defined based on the output data shown here and thus will not always order according to decile.

local storm water) are balanced with outflows (e.g., pumped water for treatment and direct use). The time series of monthly weather parameters drive the system's hydrology via a soil-moisture model embedded in WEAP. The specific model specification was based on the IEUA RUWMP, Chino Basin Optimum Management Program [*Wildermuth Environmental*, 1999], and other regional studies [e.g., *Husing*, 2006].

[36] Model calibration consisted of four main tasks: (1) tuning WEAP parameters so that modeled demand under historical climate and projected land-use and demographic assumptions match the demand forecast reported in the IEUA RUWMP; (2) tuning the Chino Basin catchment parameters so that percolation of historical precipitation and planned groundwater replenishment leads to the total basin inflow required to balance extractions according to the Chino Basin Peace I agreement [*Chino Basin Watermaster*, 2000]; (3) tuning Metropolitan import parameters so that periods of dry years trigger expected shortfalls in import deliveries; (4) tuning the upper catchment and local river flow so that local supplies vary with precipitation within the historical range described in the IEUA RUWMP. Please refer to the study of *Groves et al.* [2008a, 2008b] for details on model specification and calibration.

[37] On the basis of the modeling specification, the pathways through which climatic change can affect water management conditions in the IEUA region are: (1) irrigation requirements, (2) rates of groundwater infiltration, (3) availability of local supplies for direct use and groundwater replenishment, and (4) availability of imported supplies for direct use and groundwater replenishment. The subsections below describe the range of plausible climate change impacts upon the IUEA water management system derived from the global climate models via the Bayesian-K-nn methodology.

#### 4.1.1. Outdoor Irrigation Demands

[38] Changes in precipitation and temperature will affect outdoor irrigation demand. WEAP computes irrigation requirements for each catchment (e.g., contiguous region with similar hydrologic characteristics) by using a soil moisture algorithm [*Yates et al.*, 2005a, 2005b] that factors in monthly temperature and precipitation, crop moisture requirements (parameterized by a crop coefficient), surface runoff characteristics, soil water capacity and conductivity, and bulk parameters that specify when irrigation water is needed as a function of soil moisture. This formulation specifies that increased air temperature leads to higher potential evapotranspiration (PET) rates and greater landscape water needs. There are other potentially important effects that climate could have upon evapotranspiration not considered by the WEAP model, such as temperature effects on crops and their growing season [*Lobell et al.*, 2006] and effects of $CO_2$ on crop photosynthesis [*Kimball et al.*, 2002].

[39] Figure 9 shows traces of outdoor urban irrigation demand (including domestic and commercial landscaping), averaged over 20 weather sequences for five different climate trends (corresponding to climate change deciles 1, 3, 5, 7 and 9), assuming that all other 2005 conditions remain constant (e.g., land use patterns, demand factors, and water supply variability). The gray bars indicate the ranges of outdoor demand by year for all 180 sequences reflective of all nine climate change deciles. The figure suggests increased water demands under hotter and drier weather projections (up to an 11% increase by 2040, or an increase of 0.28 centimeters per year for decile 1) and significantly lower water demand under the wetter weather sequences (up

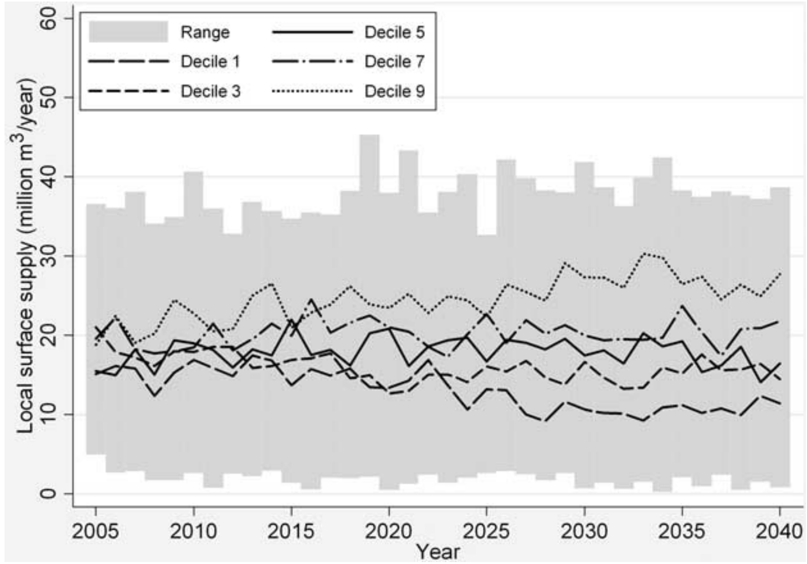


**Figure 10.** Projected local surface supply (in million cubic meter per year) for the IEUA region under different weather sequences consistent with the climate change projections from the AOGCMs. The lines indicate averages over 20 sequences for deciles 1, 3, 5, 7, and 9. The shaded bars indicate the entire range of local supply availability. Note that the deciles are defined based on the conditioning precipitation and temperature trends used in the K-nn procedure. They are not defined based on the output data shown here and thus will not always order according to decile.

to a 10% decrease by 2040, or a decrease of 0.33 centimeters per year for decile 9). The interannual variability reflected by the ranges of all annual demand projections is substantially larger than the average trends in demand. Note that in the IEUA region, these climate-induced trends would be superimposed upon rising urban water demands because of projected landscape conversion from agricultural lands and open space to urban development.

### 4.1.2. Local Supplies

[40] Trends in precipitation will change the availability of local stream flow for municipal supplies. Although a WEAP model could be constructed to explicitly model runoff to these local waterways, this application parameterizes the stream flow that are the source of local surface water supply such that during low precipitation years (as defined by the weather sequence being used) a lower supply is available for direct use and groundwater replenishment. This parameterization is tuned so that historical precipitation sequences lead to local supply availability commensurate with that observed historically (about 20 million $m^3$/year, on average).

[41] Figure 10 shows traces of local surface supplies, averaged over 20 sequences for five different climate trends (deciles 1, 3, 5, 7 and 9). The gray bars indicate the ranges of local surface supply by year for each of the 180 sequences representative of the nine climate change deciles. The range of local surface supplies for the derived weather sequences suggests decreased supplies under hotter and drier weather projections (substantial supply decreases of 42% by 2040—191 thousand $m^3$/year for decile 1) and greater supplies under the wetter weather sequences (up to a 42% increase by 2040—199 thousand $m^3$/year for decile 9). The interannual variability reflected by the ranges of all 180 local supply projections is substantially larger than the average trends in the local supply by decile.

### 4.1.3. Groundwater Infiltration

[42] Trends in precipitation could change the amount of precipitation that percolates into the underlying aquifer. The WEAP model calculates the share of monthly precipitation that (1) is evapotranspired by the land surface; (2) flows off of the catchment surface into surface streams; (3) percolates into the root-zone and flows laterally to adjacent surface streams; and (4) percolates from the root-zone into the underlying aquifer. Precipitation that percolates beyond the root zone is the primary source of inflow to the underlying Chino Groundwater basin aquifer. Groundwater replenishment using imported, recycled, and local storm water via percolation is also simulated. The model structure assumes that percolation is linearly related to precipitation.

[43] To evaluate the effects of climate change on the groundwater basin management, we simulated how the 180 climate sequences affect the Chino Basin storage assuming that development and water management patterns unfold as projected in the IEUA RUWMP (Figure 11). In these simulations the management of the Chino Basin is fixed—it does not respond to rising or declining groundwater levels. The climate sequences that exhibit positive trends in precipitation lead to increasing groundwater storage, and the climate sequences with negative precipitation treads lead to decreases in groundwater storage. Groundwater levels decline by about 15% (or 950 million $m^3$/year) under decile 1 climate sequences and increase by 13% (or 789 million $m^3$/year) under decile 9 climate sequences over the 35-year simulation period.

[44] Per the OBMP, groundwater extractions would be limited if the amount of water stored in the aquifer were to significantly decline. To evaluate how changes in pumping permits to ensure sustainability would affect overall groundwater extractions under the various climate change scenarios, the model adjusts groundwater extractions every 5 years so

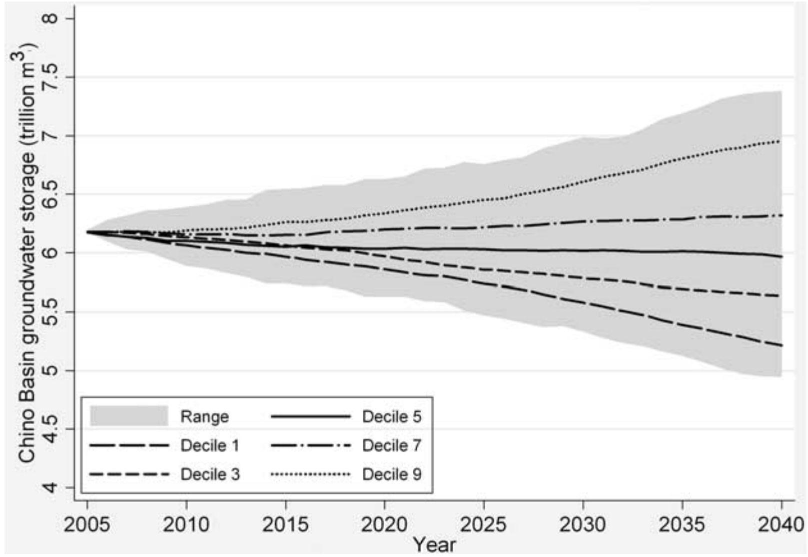


**Figure 11.** Chino Basin groundwater storage projections (trillion cubic meter) assuming no change in management under different weather sequences reflective of climate deciles 1, 3, 5, 7, and 9. Lines indicate averages across 20 sequences for each decile. The shaded region indicates the range of results across all 180 sequences (20 sequences for each of the 9 deciles). Note that the deciles are defined based on the conditioning precipitation and temperature trends used in the K-nn procedure. They are not defined based on the output data shown here and thus will not always order according to decile.

that total groundwater storage remains at the current level (about 6.2 trillion $m^3$). Figure 12 shows the projected extractions under the IEUA RUWMP assumptions (solid line) and average extractions by year for the weather sequences corresponding to climate change deciles 1, 3, 5, 7, and 9. The shaded region represents the range of all simulations. Declines in supply are due to projected groundwater pumping reductions mandated in response to falling groundwater levels. Note that restrictions are enacted or eased every five years, per the OBMP. These simulations suggest that under more severe climate change scenarios (i.e., lower climate change deciles) significant declines in allowable groundwater extractions could be mandated. Specifically, the average restrictions under deciles 1 and 3 after 2010 (when the model first evaluates the condition of the groundwater basin and adjusts allowable extractions as needed) is 30.8 million $m^3$/year

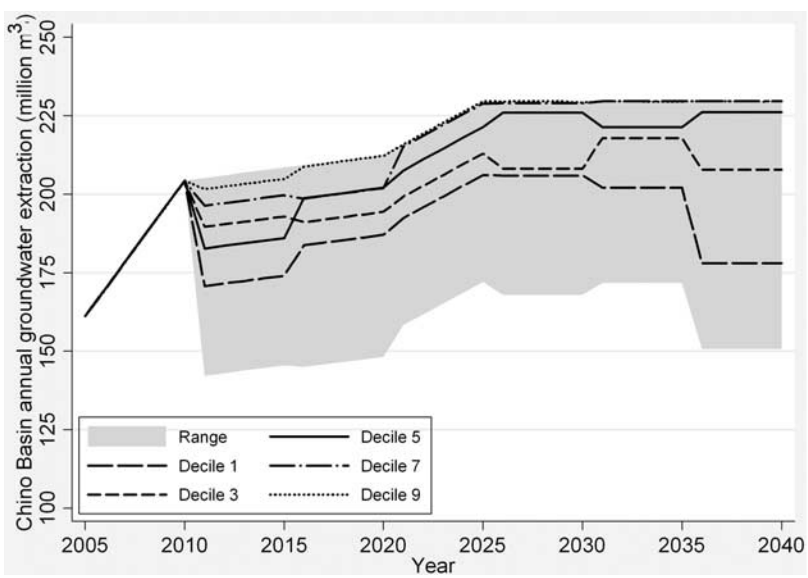


**Figure 12.** Projections of allowable groundwater extractions (million cubic meter) from the Chino Basin under climate change scenarios and adaptive groundwater management. The lines indicate average extractions (across 20 sequences) for deciles 1, 3, 5, 7, and 9. Shaded region indicates the range of results from the 180 sequences. Note that the deciles are defined based on the conditioning precipitation and temperature trends used in the K-nn procedure. They are not defined based on the output data shown here and thus will not always order according to decile.

(or 14% of the total groundwater supply) and 17.3 million $m^3$/year (or 8% of the total), respectively. Restrictions under individual plausible weather sequences are even more significant, as seen by the range results in Figure 12.

#### 4.1.4. Imports

[45] The amount of imported supply available to IEUA will also likely be affected by changed climatic conditions in the Sacramento Valley (the source region of the California State Water Project) [*Barnett et al.*, 2008; *Department of Water Resources*, 2006; *Vicuna*, 2006; *Zhu et al.*, 2005]. As this case-study did not explicitly model the hydrologic response of the Sacramento Valley river flow to climate change, we evaluate the effects of various reductions in available imports on the water management implications section below.

### 4.2. Implications for Current Management Plans

[46] We now address the question of how climate change impacts will affect the overall performance of the IEUA's water management plans. Specifically, we present how plausible climate changes, as suggested by the 21 AOGCMs and translated into local temperature and precipitation sequences using K-nn, would affect the performance of the region's current plans (i.e., the IEUA RUWMP; *IEUA* [2005]) under several levels of decline in imported supply availability. It is important to note that this approach does not explicitly consider uncertainties associated with the downscaling procedure or hydrologic modeling routines used by the WEAP model.

[47] The IEUA RUWMP's primary approach to addressing new water supply needs includes (1) increasing the use of the Chino Basin groundwater by about 75% through increased groundwater replenishment and (2) developing an extensive recycled water system to deliver up to 85 million $m^3$/year of supply by 2025 (2005 recycled deliveries totaled only about 9.9 million $m^3$). To summarize the effects that climate change would have on the performance of the region's plans with respect to supply and demand, the WEAP model calculates the average annual surplus (defined as the difference between total available water supply and total water demand) from 2021–2030 and from 2031–2040. Annual reliability is also calculated by counting the fraction of years in which the surplus is negative and subtracting that from one. Note that according to the IEUA RUWMP, the region would enjoy an excess of available supply that would grow from 17.9 million $m^3$ in 2005 to 101.3 million $m^3$ by 2025 under historical conditions.

[48] As this model does not explicitly evaluate the climate change impacts on the SWP source regions, we calculate the performance of the IEUA RUWMP under the 180 weather sequences (reflecting local changes in climate) for three levels of fixed imports: current projections, a 20% decline by 2040, and a 40% decline by 2040. These three levels were selected to represent the range of declines suggested by several recent studies that estimated the reliability of SWP deliveries under different climate change scenarios [*Department of Water Resources*, 2006; *Vicuna*, 2006; *Zhu et al.*, 2006]. Note that annual imports are also restricted during local-dry years according to the IEUA RUWMP projections for single-dry year SWP deliveries to the region.

[49] Under no climate trends and no declines in imports the average surplus is about 88.8 million $m^3$ between 2021 and 2030 and 82.6 million $m^3$ between 2031 and 2040 (top line of Table 2), and reliability is estimated to be 100%. Under declining average imports, however, the average surplus decreases to 61.7 million $m^3$ in 2030–2040 for 20% import declines and 34.5 million $m^3$ in 2030–2040 for a 40% decline in imports. Reliability decreases to 96%.

[50] Under the sequences in which precipitation increases on average (deciles 7 and 9), conditions are as good as or better than under those without climate trends (Rows 5 and 6). In these cases, increases in precipitation offset the warming increases projected under deciles 7 and 9. Decile 5, which exhibits a slightly declining precipitation and temperature increases, leads to worsening conditions for the IEUA service area when compounded with declines in imports. In the 2031–2040 time period with 20% declines in imports, the average surplus decreases by 21.0 million $m^3$ and reliability decreases to 96%. Under a 40% decline in imports, average surplus decreases to 6.8 million $m^3$ by the 2031–2040 time period and reliability decreases to 78%. Under climate changes consistent with deciles 3 and 1, the region experiences reduced reliability and significantly lower average surpluses even when there are no declines in imports. By the 2031–2040 time period, the region's supply buffer is eliminated regardless of the effects on MWD imports, and reliability decreases to less than 40% under the 20% and 40% declines in imports.

## 5. Summary and Discussion

[51] This paper describes a methodology for developing sequences of monthly local weather data that reflect regional climate trends as projected by global climate models. These sequences provide a quantitative representation of plausible climate change impacts and can be used by water management models to stress test water management plans.

[52] The methodology first develops PDFs of temperature and precipitation trends for a region from individual AOGCM results using the criteria of bias and convergence [*Tebaldi et al.*, 2005]. It then creates sequences of local weather using the K-nn bootstrapping technique [*Yates et al.*, 2003] that resamples daily historical weather data such that the future sequences have the same statistical characteristics of local weather but are consistent with the range of AOGCM-derived temperature and precipitation trends. This method overcomes the limitations accompanying an analysis that uses individual, nuanced AOGCM runs. Utilizing numerous sequences with similar underlying climate trends can be useful, as the timing and duration of droughts can make the difference between successful and unsuccessful long-term water management strategies.

[53] A key limitation of the K-nn approach as implemented here is the challenge to estimate the weighting parameter, $\delta_w^i$, that correctly biases the new weather sequences to properly reflect the AOGCM ensembles both seasonally and inter-annually. This is currently done manually, through trial-and-error. The applied method also does not guarantee that all climate impacts are accounted for nor that all possible uncertainties are addressed.

[54] The method described here provides data to support a climate impact assessment. A common approach is to evaluate management strategies against a few projections of altered climatic conditions (often including "bookend" projections). Bookend climate projections can be useful to illustrate the range of possible outcomes, but they do not

**Table 2.** Average Annual Surplus (in Million Cubic Meter) and Reliability (%, See Key) Under Different Climate Change Trends (Rows), Trends in Imports (Major Columns), and Time Periods (Minor Columns)

| Climate Change Trend | Average Annual Surplus (million m$^3$) and Reliability (see key) | | | | | |
|---|---|---|---|---|---|---|
| | No Decline in Imports | | 20% Decline in Imports by 2040 | | 40% Decline in Imports by 2040 | |
| | 2021–2030 | 2031–2040 | 2021–2030 | 2031–2040 | 2021–2030 | 2031–2040 |
| No climate trend | 89.2 | 82.8 | 75.5 | 62.0 | 60.8 | 33.9[a] |
| Decile 1 | 35.5[a] | **−12.3**[b] | 20.1[a] | **−55.5**[d] | **0.2**[b] | **−115.0**[d] |
| Decile 3 | 47.1[a] | 41.1[a] | 31.2[a] | 13.4[a] | **14.2**[b] | **−31.5**[c] |
| Decile 5 | 76.8 | 62.7 | 63.2 | 40.7[a] | 47.2[a] | **6.8**[b] |
| Decile 7 | 89.7 | 78.8 | 76.4 | 60.2 | 61.9 | 34.0[a] |
| Decile 9 | 109.3 | 102.3 | 96.8 | 83.8 | 84.2 | 65.3 |

Bold data correspond to a reliability of less than 80%.
[a]Reliability range of 80%–100%.
[b]Reliability range of 60%–79%.
[c]Reliability range of 40%–59%.
[d]Reliability range of less than 40%.

provide water managers with information about how much climate change a water agency can reasonably accommodate under different management strategies, for example.

[55] Water planners also face other important uncertainties about future conditions, and the derived climate sequences can also be combined with other assumptions about uncertain planning conditions to develop numerous scenarios. A systematic evaluation of these scenarios can help answer questions such as: "How bad must climatic changes be before our agency should invest in some new infrastructure or implement a particular water efficiency program?" and "What conditions would need to prevail for me to wish I had made alterative strategic decisions?"

[56] A key challenge is how to use these large ensembles of scenarios in a systematic decision analysis. Standard decision theory would call for the assignment of probabilities to each scenario and weighting of the results. Such an approach could lead to the identification of "optimal" water management strategies (provided that a single utility function could be defined). When the uncertainty about the future cannot be uniquely characterized by probabilistic means, however, alternative decision analytic methods may be required [*Groves and Lempert*, 2007; *Grubler and Nakicenovic*, 2001; *Hall*, 2007; *Lempert et al.*, 2004; *New et al.*, 2007; *Wack*, 1985].

[57] In the case of long-term water planning in the IEUA region, the cascading uncertainty from global greenhouse gas emissions estimates, to the global and regional climate response, to the local, downscaled hydrological response, makes it difficult to assign credible probabilistic uncertainty characterizations to changes in precipitation and temperature in the IEUA region and the source region of its imported supplies. Uncertainty about other management conditions, such as the ability for the region to aggressively expand its recycled water system, also cannot be easily characterized.

[58] Under conditions of so-called "deep uncertainty" the identification of robust solutions may be a more fruitful pursuit. Robust decision making (RDM) [*Groves and Lempert*, 2007; *Lempert et al.*, 2003, 2006] is a structured, scenario-based analytic approach for identifying solutions that perform adequately across a wide range of plausible future conditions. In brief, RDM first evaluates the performance of different strategies against a large set of scenarios. RDM then analyzes the resultant database using visualization and statistical techniques to identify conditions under which the leading strategies perform poorly. Identifying alternative strategies that are insensitive to these vulnerabilities can then help develop hedging actions to augment the promising strategies. Note that it is common to factor in cost when estimating how well a policy will fare, thus robust policies are not necessarily those that cost more. In the end, no strategy can be robust to all possible future conditions. The characterizations of vulnerabilities then provide decision makers with key tradeoff information to help them understand how a differing world view about critical uncertainties (such as climate change effects) would impact sensible choices.

[59] In this paper, the case study evaluates the implications of 180 different weather projections upon IEUA's current urban water management plan. The results showed that under drying climate sequences, outdoor water demand could increase substantially at the same time as local surface water supplies and groundwater resources become more constrained. Together, the effects would lead to reductions in the planned supply buffer and possible shortages. Compounding these local effects with declines in imports (driven by climate change or other factors in the imported water source region) would impacts IEUA water management even more.

[60] *Groves et al.* [2008a, 2008b] build on this analysis and evaluate how alternative management strategies for the IEUA region would perform against this range of plausible climate changes and other management uncertainties. Their robust decision making analysis finds that much of the IEUA region's vulnerability to climate change could be reduced by more aggressive promotion of water use efficiency in the near-term and investments in storm water capture for groundwater recharge if conditions deteriorate over the long-term. These strategies prove to be more robust than IEUA current plans because the cost of new investments are outweighed in a vast majority of the conditions evaluated by reductions in costly shortages and through the reduction in use of expensive imported supplies.

[61] These results were shown to stakeholder groups consisting of water managers and elected officials from

the IEUA region. An analysis of surveys administered before and after the presentations suggests that the participants are concerned about climate change impacts on their water system and that large scenario ensembles evaluated with RDM methods can be useful in crafting a prudent response.

[62] **Acknowledgments.** The authors of this report are grateful for the financial support received from the National Science Foundation (grant SES-0345925) and from NCAR Weather and Climate Impacts Assessment program. NCAR is sponsored by the National Science Foundation. The authors also acknowledge the modeling groups, the Program for Climate Model Diagnosis and Intercomparison (PCMDI), and the WCRP's Working Group on Coupled Modelling (WGCM) for their roles in making available the WCRP CMIP3 multimodel data set. Support of this data set is provided by the Office of Science, U.S. Department of Energy. This paper reports on work that received substantive assistance from RAND colleagues Robert Lempert, Debra Knopman, Sandra Berry, and Lynne Wainfan. The case study analysis would not have been possible without the support of Martha Davis and Richard Atwater of the IEUA.

## References

Barnett, T. P., et al. (2008), Human-induced changes in the hydrology of the western United States, *Science*, *319*, 1080–1083.
Brekke, L. D., N. L. Miller, K. E. Bashford, N. W. T. Quinn, and J. A. Dracup (2004), Climate change impacts uncertainty for water resources in the San Joaquin River Basin, California, *J. Am. Water Resour. Assoc.*, *40*(1), 149–164.
California Urban Water Agencies (2007), *Climate Change and Urban Water Resources*, 15 pp., California Urban Water Agencies, Sacramento, CA.
Chino Basin Municipal Water District v. City of Chino et al. (1978), Superior Court of the County of San Bernardino, no. 164327, 30 Jan.
Chino Basin Watermaster (2000), *Peace Agreement Chino Basin*, Chino Basin Watermaster, Rancho Cucamonga, CA.
Cleveland, W. S., and S. J. Devlin (1988), Locally weighted regression: An approach to regression analysis by local fitting, *J. Am. Stat. Assoc.*, *83*, 596–610.
Department of Water Resources (2006), *Progress on Incorporating Climate Change Into Planning and Management of California's Water Resources—Technical Memorandum Report*, California Dept. of Water Resour., Sacramento, Calif.
Fowler, H. J., S. Blenkinsop, and C. Tebaldi (2007), Linking climate change modeling to impacts studies: Recent advances in downscaling techniques for hydrological modeling, *Int. J. Climatol.*, *27*(12), 1547–1578.
Furrer, R., R. Knutti, S. R. Sain, D. W. Nychka, and G. A. Meehl (2007), Spatial patterns of probabilistic temperature change projections from a multivariate Bayesian analysis, *Geophys. Res. Lett.*, *34*, L06711, doi:10.1029/2006GL027754.
Giorgi, F., and L. O. Mearns (2002), Calculation of average, uncertainty range, and reliability of regional climate changes from AOGCM simulations via the "reliability ensemble averaging" (REA) method, *J. Clim.*, *15*, 1141–1158.
Greene, A., L. Goddard, and U. Lall (2006), Probabilistic multimodel regional temperature change projections, *J. Clim.*, *19*, 4326–4343.
Groves, D. G., and R. J. Lempert (2007), A new analytic method for finding policy-relevant scenarios, *Global Environ. Change*, *17*, 73–85.
Groves, D. G., D. Knopman, R. Lempert, S. Berry, and L. Wainfan (2008a), *Presenting Uncertainty About Climate Change to Water Resource Managers—Summary of Workshops With the Inland Empire Utilities Agency*, RAND, Santa Monica, Calif.
Groves, D. G., R. Lempert, D. Knopman, and S. Berry (2008b), *Preparing for an Uncertain Future Climate in the Inland Empire—Identifying Robust Water Management Strategies*, RAND Corporation, Santa Monica, Calif.
Grubler, A. N., and N. Nakicenovic (2001), Identifying dangers in an uncertain climate, *Nature*, *412*, 15.
Hall, J. (2007), Probabilistic climate scenarios may misrepresent uncertainty and lead to bad adaptation decisions, *Hydrol. Process.*, *21*, 1127–1129.
Huber-Lee, A., C. Swartz, J. Sieber, J. Goldstein, D. Purkey, C. Young, E. Soderstrom, J. Henderson, and R. Raucher (2006), *Decision Support System for Sustainable Water Supply Planning*, 67 pp., AWWA Research Foundation, Denver, Colo.
Husing, J. (2006), *Inland Empire Utility Agency Demand Drivers: 2004 to Build-Out*, 25 pp., Economics & Politics, Inc., Redlands, CA.
Inland Empire Utilities Agency (2005), *2005 Regional Urban Water Management Plan*, Inland Empire Utilities Agency, Chino, Calif.
Intergovernmental Panel on Climate Change (2000), *IPCC Special Report—Emissions Scenarios*, Intergovernmental Panel on Climate Change.
Intergovernmental Panel on Climate Change (2007a), *Climate Change 2007: Impacts, Adaptation and Vulnerability, Contribution of Working Group II to the Fourth Assessment Report of the Intergovernmental Panel on Climate Change*, edited by M. L. Parry et al., 976 pp., Cambridge Univ. Press, Cambridge, U.K.
Intergovernmental Panel on Climate Change (2007b), *Climate Change 2007: The Physical Scientific Basis, Contribution of Working Group I to the Fourth Assessment Report of the Intergovernmental Panel on Climate Change*, edited by S. Solomon et al., 996 pp., Cambridge Univ. Press, Cambridge, U.K. and NY.
Kilsby, C. G., P. D. Jones, A. Burton, A. C. Ford, H. J. Fowler, C. Harpham, P. James, A. Smith, and R. L. Wilby (2007), A daily weather generator for use in climate change studies, in *Environmental Modelling & Software*, pp. 1705–1719, Elsevier, Amsterdam, Netherlands.
Kim, J. W., J. T. Chang, N. L. Baker, D. S. Wilks, and W. L. Gates (1984), The statistical problem of climate inversion: Determination of the relationship between local and large-scale climate, *Mon. Weather Rev.*, *112*, 2069–2077.
Kimball, B. A., K. Kobayashi, and M. Bindi (2002), Responses of agricultural crops to free-air CO2 enrichment, *Adv. Agron.*, *77*, 293–368.
Knopman, D. S. (2006), Success matters: Recasting the relationship among geophysical, biological, and behavioral scientists to support decision making on major environmental challenges, *Water Resour. Res.*, *42*, W03S09, doi:10.1029/2005WR004333.
Lamb, P. (1987), On the development of regional climate scenarios for policy oriented climatic impact assessments, *Bull. Am. Meteorol. Soc.*, *68*, 1116–1123.
Lempert, R. J., S. W. Popper, and S. C. Bankes (2003), *Shaping the Next One Hundred Years: New Methods for Quantitative, Long-Term Policy Analysis*, 187 pp., RAND, Santa Monica, Calif.
Lempert, R., N. Nakicenovic, D. Sarewitz, and M. Schlesinger (2004), Characterizing climate-change uncertainties for decision-makers, *Clim. Change*, *65*, 1–9.
Lempert, R. J., D. G. Groves, S. W. Popper, and S. C. Bankes (2006), A general, analytic method for generating robust strategies and narrative scenarios, *Manage. Sci.*, *52*(4), 514–528.
Lobell, D., C. Field, K. Cahill, and C. Bonfils (2006), *Impacts of Future Climate Change on California Perennial Crop Yields: Model Projections With Climate and Crop Uncertainties*, 25 pp., Lawrence Livermore Natl. Lab., Livermore, CA.
Maurer, E. P. (2007), Uncertainty in hydrologic impacts of climate change in the Sierra Nevada, California under two emissions scenarios, *Clim. Change*, *82*, 9180–9189.
Miller, K., and D. Yates (2006), *Climate Change and Water Resources: A Primer for Municipal Water Providers*, 83 pp., American Water Works Association, Denver, CO.
New, M., A. Lopez, S. Dessai, and R. Wilby (2007), Challenges in using probabilistic climate change information for impact assessments: An example from the water sector, *Philos. Trans. R. Soc. London, Ser. A*, *365*, 2117–2131.
Pittock, A. B., R. N. Jones, and C. D. Mitchell (2001), Probabilities will help us plan for climate change, *Nature*, *413*, 249.
Rajagopalan, B., and U. Lall (1999), A k-nearest-neighbor simulator for daily precipitation and other variables, *Water Resour. Res.*, *35*(10), 3089–3101.
Risbey, J. S. (1998), Sensitivities of water supply planning decisions to streamflow and climate scenario uncertainties, *Water Policy*, *1*, 321–340.
Schimmelpfennig, D. (1996), Uncertainty in economic models of climate-change impacts, *Clim. Change*, *33*(2), 213–234.
Smith, R. L., C. Tebaldi, D. Nychka, and L. O. Mearns (2008), Bayesian modeling of uncertainty in ensembles of climate models, *J. Am. Stat. Assoc.*, in press.
Stakhiv, E. Z. (1998), Policy implications of climate change impacts on water resources management, *Water Policy*, *1*(2), 159–175.
Tebaldi, C., L. O. Mearns, D. Nychka, and R. L. Smith (2004), Regional probabilities of precipitation change: A Bayesian analysis of multimodel simulations, *Geophys. Res. Lett.*, *31*, L24213, doi:10.1029/2004GL021276.
Tebaldi, C., R. L. Smith, D. Nychka, and L. O. Mearns (2005), Quantifying uncertainty in projections of regional climate change: A Bayesian

approach to the analysis of multimodel ensembles, *J. Clim.*, *18*(10), 1524–1540.
Thornton, P. E., S. W. Running, and M. A. White (1997), Generating surfaces of daily meteorology variables over large regions of complex terrain, *J. Hydrol.*, *190*, 214–251.
Vicuna, S. (2006), *Predictions of Climate Change Impacts on California Water Resources Using CALSIM II: A Technical Note*, California Climate Change Center, Berkeley, CA.
Vicuna, S., E. P. Maurer, B. Joyce, J. A. Dracup, and D. Purkey (2007), The sensitivity of California water resources to climate change scenarios, *J. Am. Water Resour. Assoc.*, *43*(2), 482–498.
Wack, P. (1985), *The Gentle Art of Reperceiving—Scenarios: Shooting the Rapids* (part 2 of a two-part article), *Harvard Bus. Rev.* (November–December), pp. 2–14.
Wildermuth Environmental (1999), *Optimum Basin Management Program—Phase 1 Report*, Chino Basin Watermaster, Lake Forest, CA.
Wood, A. W., L. R. Leung, V. Sridhar, and D. P. Lettenmaier (2004), Hydrologic implications of dynamical and statistical approaches to downscaling climate model outputs, *Clim. Change*, *15*(62), 189–216.
Yates, D., S. Gangopadhyay, B. Rajagopalan, and K. Strzepek (2003), A technique for generating regional climate scenarios using a nearest neighbor algorithm, *Water Resour. Res.*, *39*(7), 1199, doi:10.1029/2002WR001769.
Yates, D., D. Purkey, J. Sieber, A. Huber-Lee, and H. Galbraith (2005a), WEAP21—A demand-, priority-, and preference-driven water planning model. part 2: Aiding freshwater ecosystem service evaluation, *Water Int.*, *30*, 501–512.
Yates, D., J. Sieber, D. Purkey, and A. Huber-Lee (2005b), WEAP21—A demand-, priority-, and preference-driven water planning model. part 1, *Water Int.*, *30*, 487–500.
Yates, D., D. Purkey, J. Sieber, A. Huber-Lee, H. Galbraith, J. West, and S. Herrod-Julius (2008), A physically-based, water resource planning model of the Sacramento Basin, California USA, *ASCE J. Water Resour. Planning Manage.*, in press.
Zhu, T., M. W. Jenkins, and J. R. Lund (2005), Estimated impacts of climate warming on California water availability under twelve future climate scenarios, *J. Am. Water Resour. Assoc.*, *14*(5), 1027–1038.
Zhu, T., M. W. Jenkins, and J. R. Lund (2006), *Estimated Impacts of Climate Warming on California Water Availability Under Twelve Future Climate Scenarios*, California Energy Commission, Sacramento, CA.

D. G. Groves, RAND Corporation, 1776 Main Street, P.O. Box 2138, Santa Monica, CA 90407-2138, USA. (groves@rand.org)

C. Tebaldi, Climate Central, One Palmer Square, Suite 330, Princeton, NJ 08542, USA.

D. Yates, Research Applications Laboratory, National Center for Atmospheric Research, 3450 Mitchell Ln., Boulder, CO 80301, USA.